CYTEK®
TRANSCEND THE CONVENTIONAL

Application Of The Cell Painting Technique On The Cytek® Amnis® ImageStream®X Mk II Imaging Flow Cytometer

Cell Painting is a method for staining critical cell organelles to establish a standard phenotypic profile for each cell type that can be used to identify normal cells from those responding to drug treatment.[1] The advantage of this approach is that a standard Cell Painting protocol can be used, circumventing the need to develop novel assays for each new compound being tested. Fluorescent dyes are applied to cells to 'paint' various cellular components, including but not limited to nucleoli, nuclei, mitochondria, the endoplasmic reticulum (ER), Golgi apparatus, and the cytoskeleton.[2] Cells are then treated with chemical or genetic perturbagens and the images analyzed to extract a large set of morphological features affected by the treatment.[1] The current method for acquiring data using the Cell Painting assay is generally through High-Content Screening (HCS), however, this method is typically applied to adherent cells in a plate-based assay. The Cell Painting method described here can be adopted for cells in suspension using the ImageStream^x system for data acquisition, allowing for characterization of a wide variety of cell types.

Herein, we demonstrate that the ImageStream^x system can be used to study the behavior of cells in suspension. To assess the feasibility of using cells in suspension with the Cell Painting assay, cells from the K562 cell line were treated with varying doses of the drug phenformin. Phenformin is a biguanide formerly used in the treatment of diabetes and was removed from the pharmaceutical market due to a high propensity to induce lactic acidosis through the inhibition of mitochondrial complex I.[3,4] Untreated and treated K562 cells were stained with CD45, SYTO™ 14 (nucleoli/RNA), MitoTracker™ Orange (MTO, mitochondria), concanavalin A (ConA, endoplasmic reticulum), wheat germ agglutinin (WGA, Golgi plasma membrane), phalloidin (actin filaments), and Hoechst (DNA) to identify various cellular components. IDEAS® image analysis software with the Machine Learning module was employed to create a custom classifier that combines features for identifying subcellular components exhibiting the greatest response to phenformin, to quantify cell morphological changes, and establish the phenotype profile of cells before and after drug treatment.

Materials & Methods

Materials

This study was conducted using the lymphoblastic cell line K562 from the American Type Culture Collection. Hanks' Balanced Salt Solution (HBSS), bovine serum albumin, and phosphate buffered saline were obtained from Fisher Scientific. 10% formaldehyde, methanol free ultrapure stock solution was procured from Polysciences. Phenformin, the drug used to induce changes in cell morphology, and the permeabilization reagent Triton X 100 (Tx100) was purchased from MilliporeSigma. Details on the staining reagents and antibodies are outlined in the table on the next page. Cells were treated and stained according the sample acquisition section below.

Figure 1

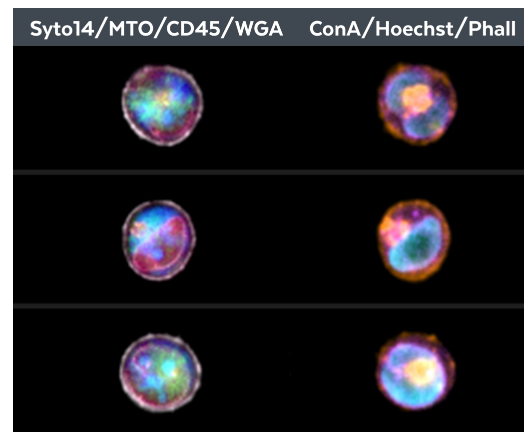

Figure 1: Sample image gallery display of K562 cells acquired at 40X magnification with overlay images of SYTO14 (blue)/MTO (green)/WGA (magenta) in column 1 and ConA (purple)/Hoechst (blue)/Phalloidin (orange) in column 2.

Feature	Fluorochrome	Target	Channel	Supplier
SYTO14	N/A	Nucleoli/RNA	2	Life Technologies
MitoTracker Orange (MTO)	N/A	Mitochondria	3	Life Technologies
Concanavalin A (ConA)	AF594	Endoplasmic Reticulum	4	Life Technologies
CD45	PECy5	WBC Surface	5	BioLegend
Hoechst 33342	N/A	DNA	7	Life Technologies
Wheat Germ Agglutinin (WGA)	AF647	Golgi Plasma Membrane	11	Life Technologies
Phalloidin	AF750	Actin Filaments	12	Life Technologies

Antibody Cocktail

Initial staining was performed using an antibody cocktail prepared in 50 µl of HBSS with MitoTracker Orange and CD45 PE-Cy7. The secondary antibody cocktail was prepared in 100 µl of permeabilization buffer (PBS 0.1%Tx100) SYTO14, ConA AF594, WGA AF647 and phalloidin AF750. Finally, the cells were prepared in 25 µl of PBS with 1% formalin and Hoechst 33342.

Preparation

K562 cells were cultured at 0.4 x 10^5 cells/mL without (0 mM) and with (0.1 mM – 2.0 mM) phenformin for 72 hours. After incubation, cells were washed with 1X phosphate-buffered saline (PBS)/0.25% bovine serum albumin (BSA) wash buffer (WB) and centrifuged at 200 x g for 5 minutes. The cell pellets were resuspended in 50 µL of prewarmed HBSS buffer and stained with MitoTracker Orange and CD45 PE-Cy7. Cells were incubated for 30 minutes at 37°C. After incubation, cells were washed and centrifuged. Cell pellets were then fixed with 4% formalin and incubated for 20 minutes, washed and centrifuged. Cell pellets were resuspended in 100 µL of permeabilization buffer and a staining cocktail comprised of SYTO 14, ConA AF594, WGA AF647, and phalloidin AF750.

Cells were incubated for 30 minutes, washed with permeabilization buffer, and centrifuged. Cell pellets were resuspended in 25 µL of 1% formalin and stained with Hoechst 33342. Samples were then acquired on the ImageStream^X system.

Sample Acquisition

Samples were collected at either 40X or 60X magnification. Side scatter (SSC), 405 nm, 488 nm, 561 nm, and 642 nm laser settings were evaluated and set using processed K562 cells. One thousand cell events were collected for compensation samples with brightfield (BF) and SSC off, while 10,000 cell events of fully stained samples were collected with BF and SSC turned on. Data analysis was performed using the IDEAS image analysis software.

Results

Samples were initially analyzed using the Apoptosis Wizard in the IDEAS image analysis software. Wizards greatly simplify analysis by guiding the user through each critical step and automatically adding the appropriate plots. The wizard began by optimizing the image gallery display properties for each fluorochrome used in the experiment. Next, in-focus cells were identified using the Gradient RMS Ch01 histogram where higher Gradient RMS values equated to sharper, better quality images of cells. Single cells were then detected with an Area Ch01 vs. Aspect Ratio Ch01 plot and gated to exclude cell doublets, debris, and clumps. Intensity plots were created for individual fluorochromes to isolate positive cells for each marker. Finally, apoptotic cells were characterized with a dot plot of DNA Contrast vs. DNA Area Threshold 50%, and the apoptotic index was measured using a region on the plot. Figure 2 presented images of single cells for each of the markers used in the Cell Painting assay.

Figure 2

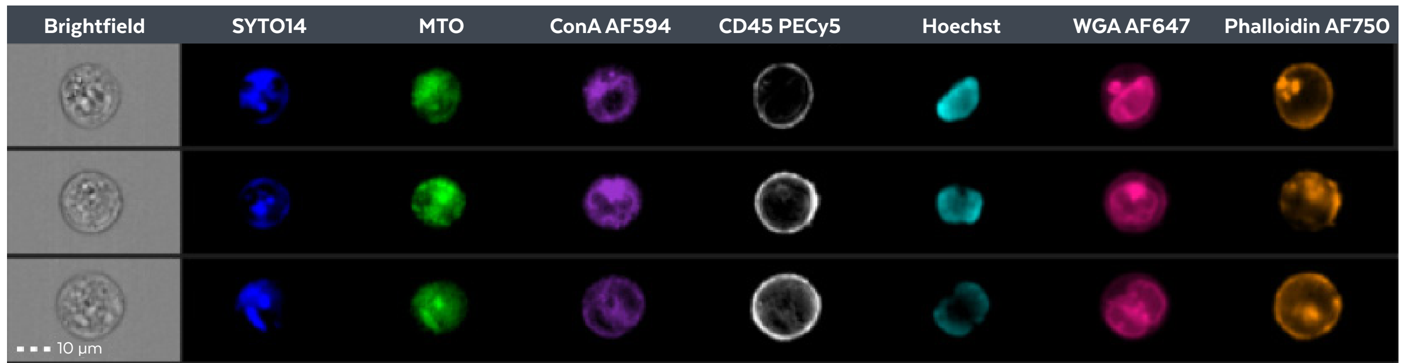

Figure 2: Image gallery display of BF, and fluorescent images of SYTO 14, MTO, ConA AF594, CD45 PE-Cy5, Hoechst, WGA AF647, and phalloidin AF750 staining at 40X magnification.

Phenformin treated and untreated K562 cells were assayed to determine if effects to mitochondria were detectable on the ImageStream[x] system. A dose-response curve was created with the mean value of the Bright Detail Intensity R3 feature for MTO and examined at each dose to determine if there were variations in the intensity of localized bright spots in the images between doses, and if those intensity variations in images increased with higher doses (Figure 3).

Figure 3

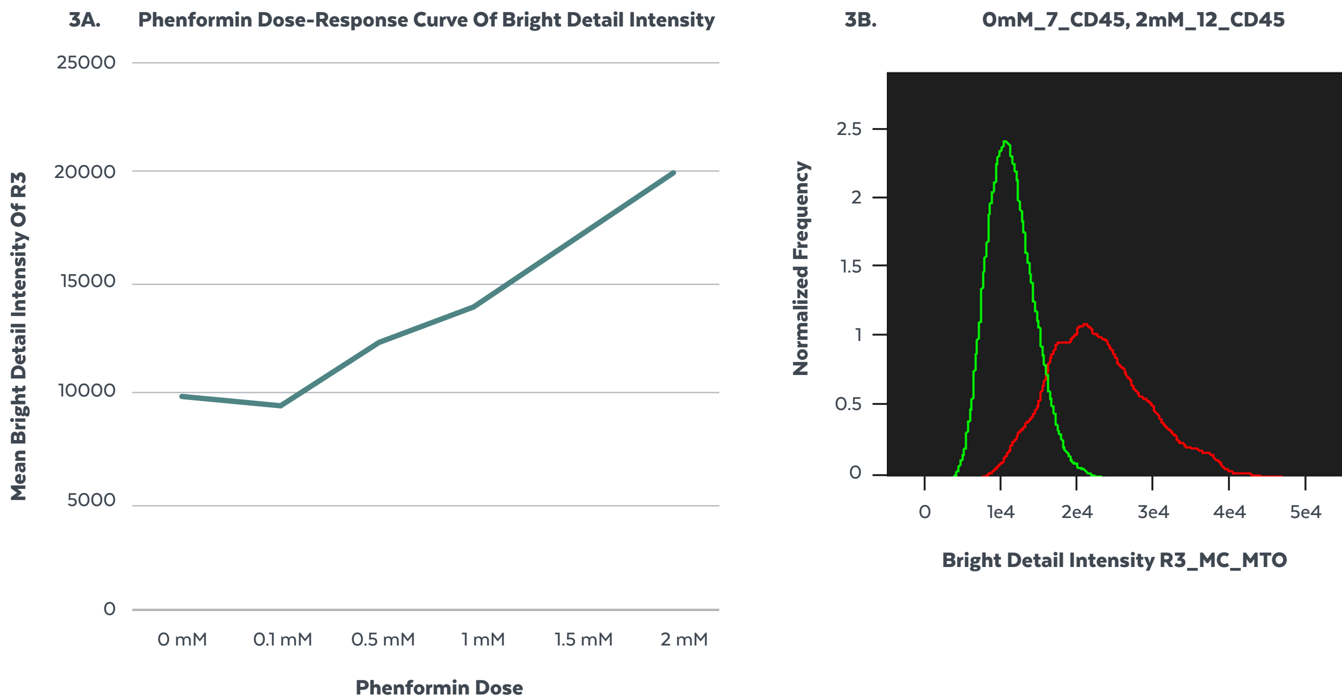

Figure 3A: Phenformin dose-response curve plotting the mean Bright Detail Intensity of R3 feature for MTO. **3B)** Histogram Bright Detail Intensity comparison of untreated (green) vs. 2.0 mM phenformin treated (red) samples.

To determine the highest comparison dose, the post-processing apoptotic cell count of dosages between 0 mM and 2.0 mM was examined using the IDEAS software Apoptosis Wizard (Figure 4).

Figure 4

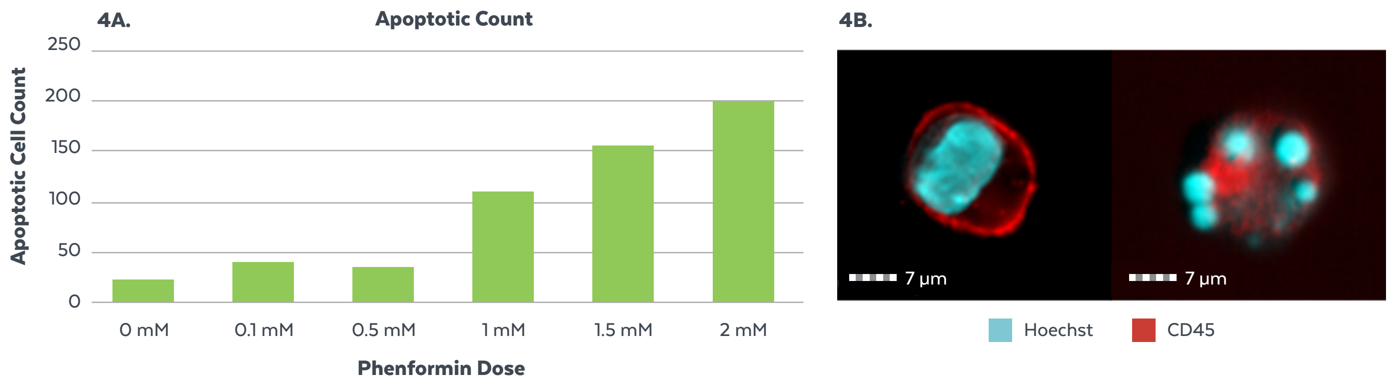

Figure 4A: Apoptotic cell count for each phenformin dose. **4B)** Image comparison of untreated vs. 2.0 mM phenformin treated samples displaying increased nuclear fragmentation and granularity in the treated cells.

Next, the Machine Learning module was used to screen 2,810 features, 62 of which were found to contribute to maximizing separation between the treated (2.0 mM phenformin) and untreated (0 mM phenformin) samples using the Fisher's Discriminant Ratio (R_d). A dose-response curve plotting the mean ML Classifier for each sample was created (Figure 5) and demonstrates an increased response to increased dosages of phenformin.

Figure 5

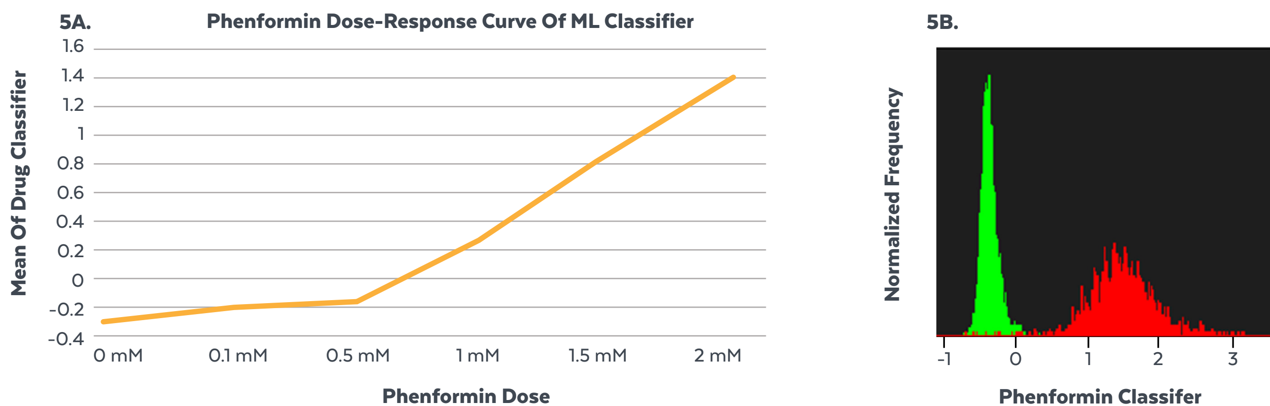

Figure 5A: Phenformin dose-response curve plotting the mean value of the custom ML classifier displaying an increased response with increasing dosages. **5B)** Histogram overlay of ML classifier comparison of untreated (green) to 2mM Phenformin (red).

Changes between the treated and untreated samples identified from the Machine Learning classifier are listed in Table 6B, with representative images showing a dramatic increase in texture, aggregates, granules and nuclear fragmentation after phenformin treatment Figure 6. The major morphological differences occurred in the nucleus, nucleoli/RNA, mitochondria, and ER.

Figure 6

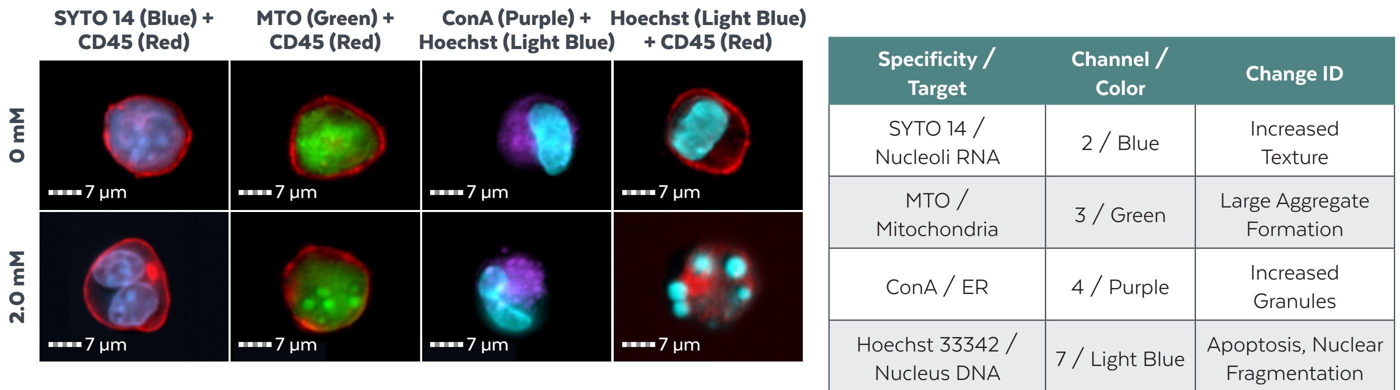

Specificity / Target	Channel / Color	Change ID
SYTO 14 / Nucleoli RNA	2 / Blue	Increased Texture
MTO / Mitochondria	3 / Green	Large Aggregate Formation
ConA / ER	4 / Purple	Increased Granules
Hoechst 33342 / Nucleus DNA	7 / Light Blue	Apoptosis, Nuclear Fragmentation

Figure 6: Images of untreated (0 mM) vs. treated (2.0 mM) cells in corresponding to the changes identified. Images were captured at 60X magnification.

Figure 7

Feature	Weight %
Max Pixel_MC_Ch07 Hoechst	2.49
Raw Max Pixel_MC_Ch07 Hoechst	2.49
Mean Pixel_Threshold(M07, Ch07 Hoechst, 30%)_Ch07 Hoechst	2.34
Mean Pixel_M07_Ch07 Hoechst	2.2
Mean Pixel_Object(M07, Ch07 Hoechst, Tight)_Ch07 Hoechst	2.2
Std Dev_M07_Ch07 Hoechst	2.19
Mean Pixel_Morphology(M07, Ch07 Hoechst)_Ch07 Hoechst	2.16
Std Dev_Object(M07, Ch07 Hoechst, Tight)_Ch07 Hoechst	2.15
Intensity_MC_Ch07 Hoechst	2.12
Intensity_Object(M07, Ch07 Hoechst, Tight)_Ch07 Hoechst	2.11
Max Pixel_Skeleton(Morphology(M07, Ch07 Hoechst), Ch07 Hoechst, Thin)_Ch07 Hoe	2.07
Mean Pixel_Skeleton(Morphology(M07, Ch07 Hoe), Ch07 Hoe, Thin)_Ch07 Hoe	2.06
Std Dev_Morphology(M07, Ch07 Hoechst)_Ch07 Hoechst	2.06
Intensity_Threshold(M07, Ch07 Hoechst, 70)_Ch07 Hoechst	1.98
Modulation_M07_Ch07 Hoechst	1.97
Min Pixel_Skeleton(Morphology(M07, Ch07 Hoechst), Ch07 Hoechst, Thin)_Ch07 Hoe	1.82
Max Pixel_Skeleton(Object(M07, Ch07 Hoechst, Tight), Ch07 Hoechst, Thin)_Ch07 Hoe	1.79
Intensity_Threshold(M07, Ch07 Hoechst, 50)_Ch07 Hoechst	1.77
Max Pixel_Skeleton(M07, Ch07 Hoechst, Thin)_Ch07 Hoechst	1.77
Mean Pixel_Skeleton(M07, Ch07 Hoechst, Thin)_Ch07 Hoechst	1.73
Mean Pixel_Skeleton(Object(M07, Ch07 Hoechst, Tight), Ch07 Hoechst, Thin)_Ch07	1.73
Max Pixel_MC_Ch02 SYTO14	1.68
Raw Max Pixel_MC_Ch02 SYTO14	1.68
Modulation_Object(M07, Ch07 Hoechst, Tight)_Ch07 Hoechst	1.66
Mean Pixel_Threshold(M02, Ch02 SYTO14, 30%)_Ch02 SYTO14	1.65
Std Dev_M02_Ch02 SYTO14	1.59
Mean Pixel_Morphology(M02, Ch02 SYTO14)_Ch02 SYTO14	1.59
Max Pixel_Skeleton(Morphology(M02, Ch02 SYTO14), Ch02 SYTO 14, Th)_Ch02 SYTO14	1.58
Mean Pixel_Object(M02, Ch02 SYTO14, Tight)_Ch02 SYTO14	1.58
Mean Pixel_M02_Ch02 SYTO 14	1.55
Std Dev_Morphology(M02, Ch02 SYTO14)_Ch02 SYTO14	1.54

Feature	Weight %
Median Pixel_M07_Ch07 Hoechst	1.53
Min Pixel_Skeleton(M07, Ch07 Hoechst, Thin)_Ch07 Hoechst	1.53
Std Dev_Object(M02, Ch02 SYTO14, Tight)_Ch02 SYTO14	1.53
Max Pixel_Skeleton(Object(M02, Ch02 SYTO14, Tight), Ch02 SYTO14, Th)_Ch02 SYTO14	1.53
Max Pixel_Skeleton(M02, Ch02 SYTO14, Thin)_Ch02 SYTO14	1.53
Mean Pixel_Skeleton(M02, Ch02 SYTO14, Thin)_Ch02 SYTO14	1.45
Mean Pixel_Skeleton(Object(M02, Ch02 SYTO14, Tight), Ch02 SYTO14 Th)_Ch02 SYTO14	1.44
Max Pixel_Valley(M02, Ch02 SYTO14 3)_Ch02 SYTO14	1.42
Min Pxel_Skeleton(Object(M07, Ch07 Hoechst, Tight), Ch07 Hoechst, Thin)_Ch07 Hoe	1.42
Mean Pixel_Skeleton(Morphology(M02, Ch02 SYTO14), Ch02 SYTO14, Th)_Ch02	1.41
Mean Pixel_Peak(M03, Ch03 MTO, Bright, 15)_Ch03 MTO	1.38
Median Pixel_Peak(M03, Ch03 MTO, Bright, 15)_Ch03 MTO	1.37
Spot Intensity Min_Peak(M03, Ch03 MTO, Bright, 15)_Ch03 MTO	1.37
Max Pixel_Valley(Object(M02, Ch02 SYTO14, Tight), Ch02 SYTO14, 3)_Ch02 SYTO14	1.37
Median Pixel_M02_Ch02 SYTO14	1.34
Spot Intensity Max_Peak(M03, Ch03 MTO Bright, 15)_Ch03 MTO	1.32
Max Pixel_Peak(M03, Ch03 MTO, Bright 15)_Ch03 MTO	1.31
Intensity_Threshold(M07, Ch07 Hoechst, 30)_Ch07 Hoechst	1.31
Modulation_M02_Ch02 SYTO14	1.23
Max Pixel_Valley(Morphology(M02, Ch02 SYTO 14), Ch02 SYTO14, 3)_Ch02 SYTO14	1.2
Min Pexal_Skeleton(M02, Ch02 SYTO14, Thin)_Ch02 SYTO14	1.2
Bright Detail Intensity R3_MC_Ch02 SYTO14	1.2
Bright Detail Intensity R3_Threshold(M07, Ch07 Hoechst, 30%)_Ch07 Hoechst	1.17
Modulation_Object(M04, Ch04 ConA, Tight)_Ch04 ConA	1.17
Bright Detail Intensity R3_Threshold(M04, Ch04 ConA, Tight)_Ch04 ConA	1.16
Bright Detail Intensity R3_Threshold(M07, Hoechst, 50%)_Ch07 Hoechst	1.14
Min Pixel_Skeleton(Object(M02, Ch02 SYTO14, Tight), Ch02 SYTO14, Th)_Ch02 SYTO14	1.14
Std Dev_Object(M04, Ch04 ConA, Tight)_Ch04 ConA	1.14
Max Pixel_MC_Ch04 ConA	1.13
Raw Max Pixel_MC_Ch04 ConA	1.13
Bright Detail Intensity R3_Threshold(M07, Ch07 Hoechst, 70)_Ch07 Hoechst	1.12

Figure 7: Sixty-two features were identified that maximized separation between drug-treated and untreated samples. Purple highlighted features relate to the nucleus, green highlighted features relate to nucleoli/RNA, yellow highlighted features relate to mitochondria, and red highlighted features relate to the ER.

Summary

The Cell Painting assay is a powerful tool for drug discovery to help uncover targeted therapeutic effects of countless compounds. The ImageStream^x imaging flow cytometer can successfully measure dose dependent effects of drug treatments on cells in suspension using the standard Cell Painting assay. With the IDEAS software Machine Learning module, organelles affected by drug treatment were identified and the affected features were ranked based on their R_d value. This process can lead investigators to determine which compounds should be more closely evaluated for novel drug discovery.

References

1. Bray MA, Singh S, Han H, Davis CT, Borgeson B, Hartland C, Kost-Alimova M, Gustafsdottir SM, Gibson CC, Carpenter AE. Cell painting, a high-content image-based assay for morphological profiling using multiplexed fluorescent dyes. Nat Protoc. 2016 Sep;11(9):1757-74. doi: 10.1038/nprot.2016.105. PMID: 27560178; PMCID: PMC5223290.
2. Gustafsdottir SM, Ljosa V, Sokolnicki KL, Anthony Wilson J, Walpita D, Kemp MM, Petri Seiler K, Carrel HA, Golub TR, Schreiber SL, Clemons PA, Carpenter AE, Shamji AF. Multiplex cytological profiling assay to measure diverse cellular states. PLoS One. 2013 Dec 2;8(12):e80999. doi: 10.1371/journal.pone.0080999. PMID: 24312513; PMCID: PMC3847047.
3. Kwong SC, Brubacher J. Phenformin and lactic acidosis: a case report and review. J Emerg Med. 1998 Nov-Dec;16(6):881-6. doi: 10.1016/s0736-4679(98)00103-6. PMID: 9848705.
4. Weinberg SE, Chandel NS. Targeting mitochondria metabolism for cancer therapy. Nat Chem Biol. 2015 Jan;11(1):9-15. doi: 10.1038/nchembio.1712. PMID: 25517383; PMCID: PMC4340667.

For Research Use Only. Not for use in diagnostic or therapeutic procedures.

© 2026 Cytek Biosciences, Inc. All rights reserved. Cytek, the Cytek Logo, Amnis, ImageStream, and IDEAS are trademarks of Cytek Biosciences, Inc. All other service marks, trademarks and tradenames are the property of their respective owners.

N9-20158 Rev. A
March 2026